APPLICATION OF A MODEL OF HYDROGEN-ASSISTED FATIGUE CRACK GROWTH IN 4130 STEEL*

R. L. AMARO
Colorado School of Mines
Golden, Colorado USA
A. J. SLIFKA
National Institute of Standards and
Technology
Boulder, Colorado USA

B. E. LONG
Colorado School of Mines
Golden, Colorado USA
E. S. DREXLER
National Institute of Standards and
Technology
Boulder, Colorado USA

D. T. O'CONNOR
National Institute of Standards and
Technology
Boulder, Colorado USA

ABSTRACT

In this work, we applied a finite element model to predict the cyclic lifetime of 4130 steel cylinders under the influence of hydrogen. This example is used to demonstrate the efficacy of a fatigue crack growth (FCG) model we have developed. The model was designed to be robust and incorporate features of stress-assisted hydrogen diffusion, large-scale plasticity, hydrogen gas pressure, loading frequency, and effects of microstructure. The model was calibrated to the 4130 steel material by use of tensile tests and experimental FCG results of a compact tension specimen. We then used the model to predict the hydrogen-assisted FCG rate and cycle life of a pressurized cylinder with a deliberate initial thumbnail crack. The results showed good correlation to the cyclic lifetime results of 4130 pressurized cylinders found in the literature.

INTRODUCTION

If hydrogen is to be used as an energy carrier to provide an alternative to fossil fuels, a vast network of pipelines is required to transport the hydrogen across the country. Furthermore, truck-mounted and loose pressure vessels will likely continue to be employed as short-distance hydrogen transportation and storage solutions. Steel pipelines are likely the most economical means of long-distance hydrogen transportation. The most common materials used in natural gas pipelines are API-5L grade steels that have a specified minimum yield stresses between 52 ksi (358 MPa) and 80 ksi (551 MPa). These steels carry the designation of API-5L X52, X65, X70, X80, etc. Future hydrogen-specific pipe installations may include the use of X100 and X120 pipeline steels. Pressure vessels for hydrogen use are commonly produced with ASTM SA/A516 or AISI 413X steels, where the X is replaced with a 0 or 5 depending upon carbon content. While the difference in geometries and boundary conditions between pipes and the cylinder portion of pressure vessels may be easily represented, the steels used comprise vastly different microstructures. Although the differing microstructures

605

may or may not yield significantly different deformation responses under normal operating conditions, they do likely produce varying hydrogen diffusivities [1-4] and, therefore, have the potential for significantly different fatigue and fracture responses in the presence of hydrogen.

The pipeline and infrastructure required to transport hydrogen across the United States does not currently exist. Given that steel pipelines have for a long time been the best method to transport fuels long distances, the United States will need a hydrogen transmission network similar to that of the current natural gas transmission network in size. The United States currently has approximately 305,000 miles of natural gas pipelines [5] and only one half of one percent of that quantity is hydrogen-dedicated pipeline [6, 7]. A primary barrier to the use of carbon steel to transport hydrogen, whether by pipeline or pressure vessel, is the deleterious effect that hydrogen has upon the deformation, fracture, and fatigue response of the steel [8, 9]. Design and engineering codes for hydrogen transmission via pipeline [10] and distribution via piping [11], as well as pressure vessels [12], have been developed to ensure safe and effective use of these steels for hydrogen service. The newest versions of the codes that support the transmission and distribution of hydrogen and hydrogen-bearing gasses are being informed by the recent experimental results from laboratories such as the National Institute of Standards and Technology (NIST) and Sandia National Laboratories (SNL) [13-15]. It is nearly universally understood that microstructure-specific physics-based models are required to inform the large-scale infrastructure expansion required to meet the needs of a future network for hydrogen transmission.

A phenomenological hydrogen-assisted fatigue crack growth (HA-FCG) model that predicts cycles to failure for given material-specific calibration parameters and known initial and boundary conditions has been created and used to inform the forthcoming 2016 version of the ASME B31.12 Hydrogen Piping and Pipeline code (to be released in 2017). The current HA-FCG model is based upon the understanding that the crack-growth response of a steel results from an interaction between competing damage mechanisms and was initially implemented with closed-form solutions to the crack stress response and the stress-assisted hydrogen diffusion [16, 17]. In our current effort, the elastic-plastic deformation response coupled with the hydrogen diffusion model is implemented in the finite element (FE) program ABAQUS[1]. The predicted hydrogen concentration, as a function of elastic and plastic deformation and gas pressure, is coupled with the existing phenomenological framework to predict the HA-FCG response of the steel. The strength of this modeling framework is that one can predict a steel's HA-FCG response, for any geometry that can be modeled, based upon laboratory results from simple specimens, e.g. compact tension (CT) specimens. This work details the use of the modeling framework to predict cycles to failure for pipes and pressure vessels that have thumbnail-shaped internal cracks. Ultimately, the model implementation will be updated to include

---

[1] Identified for clarity only, no endorsement by NIST is implied

microstructure-specific steel domains and their associated deformation and hydrogen diffusion properties.

Coupled Hydrogen-Assisted Fatigue Crack Growth Model

The phenomenological HA-FCG model, calibrated to X100 pipeline steel is detailed in [16, 17]. The model has also been partially calibrated to X52 and X70 steels [18]. The model has the following functional form:

$$\frac{da}{dN}_{\text{total}} = \frac{da}{dN}_{\text{fatigue}} + \delta\left(P_{\text{H}} - P_{\text{H}_{\text{th}}}\right)\frac{da}{dN_{\text{H}}},$$ EQ. 1

where, a is the crack length, N is the number of cycles, and P is the hydrogen pressure. The model predicts the total fatigue crack growth as the sum of the fatigue crack growth resulting from fatigue only and the HA-FCG. HA-FCG is predicted by

$$\frac{da}{dN_{\text{H}}} = \left[\left(\frac{da}{dN_{P_{\text{H}}}}\right)^{-1} + \left(\frac{da}{dN_{\Delta K}}\right)^{-1}\right]^{-1}.$$ EQ. 2

Equation 2 predicts that the HA-FCG results from a competitive interaction between a hydrogen-pressure-dominated component, $\frac{da}{dN_{P_{\text{H}}}}$, and a component dominated by hydrogen-assistance from the crack-extension driving force, $\frac{da}{dN_{\Delta K}}$. The hydrogen-pressure-dominated FCG term is defined as

$$\frac{da}{dN_{P_{\text{H}}}} = a1\Delta K^{B1}(C_{\text{L}})^{d1},$$ EQ. 3

where ΔK is the stress intensity range, C_{L} is the spatial and time-dependent lattice hydrogen concentration determined from ABAQUS, and $a1$, $B1$, and $d1$ are fitting parameters. The component dominated by hydrogen-assistance from the crack-extension driving force is defined as

$$\frac{da}{dN_{\Delta K}} = a2\Delta K^{B2}(C_{\text{L}})^{d2},$$ EQ. 4

and $a2$, $B2$, and $d2$ are fitting parameters.

The lattice hydrogen concentration, C_{L}, is predicted by use of a new user-defined material (UMAT) model that we developed in ABAQUS called H-diff. The UMAT H-diff is based upon the architecture of the existing high-temperature material model UMATHT as in [19]. In order to account for hydrogen trapping by dislocations, H-diff utilizes the extended Fick's law provided in [20]. The elastic-plastic material response is predicted by the Ramberg-Osgood (RO) constitutive model by use of the ABAQUS "Deformation Plasticity" parameters. The R-O model,

$$\frac{\varepsilon}{\varepsilon_0} = \frac{\sigma}{\sigma_0} + \alpha\left(\frac{\sigma}{\sigma_0}\right)^n,$$ EQ. 5

calculates the total strain, ε, as a function of the total stress, σ, or vice versa. The parameters ε_0 and σ_0 are the strain and stress at yielding, respectively, and α and n are constants. The hydrogen concentration is calculated via the hydrogen transport equation of [21] and modified by [20]

$$\frac{D}{D_{\text{eff}}}\frac{\partial C_{\text{L}}}{\partial t} = D\nabla^2 C_{\text{L}} - \nabla\cdot\left(\frac{DV_{\text{H}}}{3RT}C_{\text{L}}\nabla\sigma_{\text{h}}\right) - \left(\sum_j \eta^j \theta_T^j \frac{\partial N_T^j}{\partial \varepsilon^{\text{p}}}\right)\frac{\partial \varepsilon^{\text{p}}}{\partial t}.$$ EQ. 6

The parameters that are required in order to solve for the hydrogen concentration are defined as follows: D is the hydrogen diffusion coefficient, D_{eff} is the effective

diffusion coefficient, C_L is the hydrogen concentration in the normal interstitial lattice site (NILS), V_H is the partial molar volume of hydrogen, R is the universal gas constant, T is the absolute temperature, σ_h is the hydrostatic stress, η is the number of trapping sites per trap type j, θ_T is the trap site occupancy for a given trap site j, N_T is the trap-site density for a given trap site j, ε^p is the equivalent plastic strain and the ∇ is the mathematical vector differential operator. Equation 6 is an extension of Fick's law that incorporates the influence of both hydrostatic stress and plastic strain on hydrogen transport. The hydrogen concentration equation has the capability to solve for the hydrogen concentration in the lattice and three separate trap sites. This implementation is concerned with only the weakly-trapped hydrogen, in which case the model only determines the hydrogen diffusion resulting from NILS and dislocations. Oriani's theory [22] provides the relationship between the trap-site occupancies, θ_T^j, and the lattice-site occupancies, θ_L, as

$$\frac{\theta_T^j}{1-\theta_T^j} = \frac{\theta_L}{1-\theta_L} \, exp\left(\frac{W_B^j}{RT}\right), \qquad \text{EQ. 7}$$

where W_B^j is the trap binding energy for the trap of interest (dislocations in this case). The hydrogen concentration in the NILS and the trap sites is given by EQ. 8 and EQ. 9, respectively.

$$C_L = \beta N_L \theta_L \qquad \text{EQ. 8}$$

$$C_T^j = \eta^j N_T^j \theta_T^j \qquad \text{EQ. 9}$$

Literature values are used for the number of interstitial sites per atom, β, the number of solvent atoms per unit volume, N_L, and the number trap sites per trap type, η^j. The trap densities for a given trap type, N_T^j, taken here as only the trap density for dislocations, is solved as a function of equivalent plastic strain per the work of [23]. The relationship is given in EQ. 10

$$N_T^{\text{dislocations}} = \frac{10^{23.26-2.33exp\left(-5.5\varepsilon^p\right)}}{N_A}, \qquad \text{EQ. 10}$$

where N_A is Avogadro's constant. Finally, the effective hydrogen diffusion is calculated by use of

$$\frac{D}{D_{\text{eff}}} = 1 + \sum_j \frac{\partial C_T^j}{\partial C_L}. \qquad \text{EQ. 11}$$

Equations 6 through 11 are solved at each integration point and at each time step within the new user-defined material model H-Diff.

**HA-FCG Calibration to a 4130 Pressure Vessel Steel**

The data in [24] are leveraged here to calibrate the elastic-plastic constitutive behavior, the HA-FCG response and the diffusivity parameters. The R-O parameters and the hydrogen diffusion parameters are provided in Tables 1 and 2, respectively. The experimental HA-FCG results of the 4130 steel [25] are provided in Fig. 1(a).

Table 1: Ramberg-Osgood parameters for 4130 steel

Material	ε_0	σ_0 (MPa)	α	n
4130	0.0034	762	0.58	20

Table 2: Model input data for hydrogen diffusion

D (m^2/s)	V_H (m^3/mol)	N_L (mol/m^3)	W_B (J/mol)	β	η
1.5×10^{-8}	2.0×10^{-6}	8.46×10^5	6.1×10^4	1	1

(a)   **(b)**
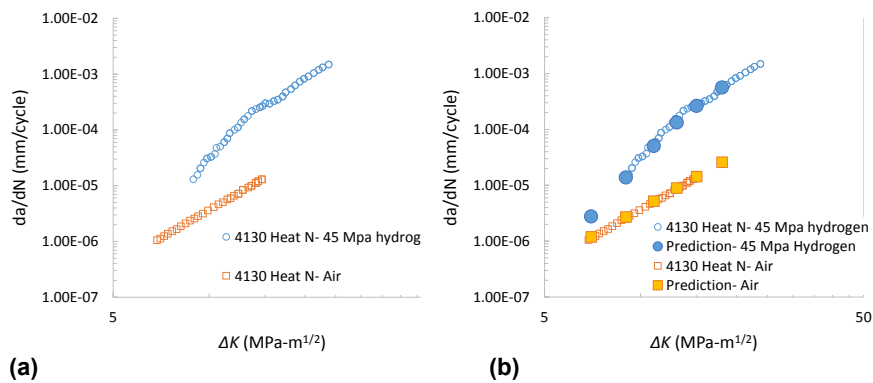
Figure 1: (a) Experimental HA-FCG results for 4130 steel in air and 45 MPa gaseous hydrogen [25], (b) experimental and predicted HA-FCG results for 4130 steel in air and 45 MPa hydrogen gas.

A one-half symmetry CT specimen was modeled in ABAQUS to elucidate the predictive capabilities of the model for HA-FCG of 4130 steel. The coupled deformation-hydrogen diffusion parameters are provided in Table 2. Figure 1(b) shows the predicted HA-FCG results of the 4130 CT specimen in 45 MPa gaseous hydrogen, a frequency of 1 Hz, and a load ratio of R=0.1. The fatigue crack growth values were predicted at ΔK values of 7 MPa-m$^{0.5}$, 9 MPa-m$^{0.5}$, 11 MPa-m$^{0.5}$, 13 MPa-m$^{0.5}$, and 15 MPa-m$^{0.5}$. The predicted data is overlaid upon the experimental data of [25]. Analysis of the predictions in Fig. 1(a) indicate that the coupled model predicts HA-FCG within a factor of $\pm$ 1.5 and is deemed to be sufficiently calibrated to HA-FCG of 4130 steel. Of interest, then, is to use the model implementation on realistic geometries. To do so, this work leverages the results of [26], in which 4130 pressure vessels with engineered flaws of known size, semi-elliptical shape with nominal root radius 0.5 mm and an aspect ratio (a/2c) of 1/3 aligned along the length of the cylinder, are cycled from 3.5 MPa (500 psi) to 43.8 MPa (6350 psi) until failure. A finite element model of the pressure vessel, which incorporates extensive symmetry boundary conditions, was created in ABAQUS and is shown in Fig. 2a.

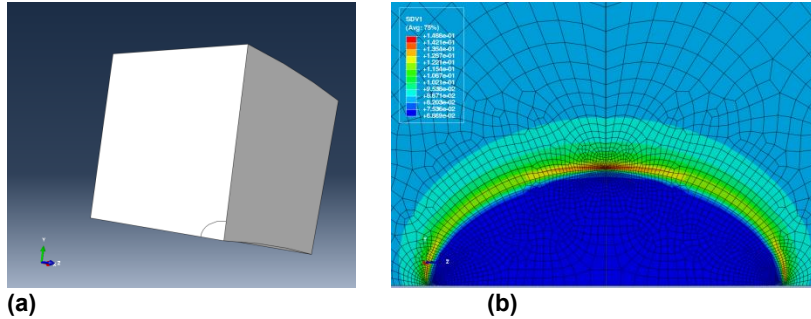**(a)**   **(b)**

Figure 2: (a) Pressure vessel FE model with thumbnail-shaped crack, (b) predicted hydrogen concentration at the crack tip resulting from 43.8 MPa internal hydrogen pressure. Thumbnail-shaped crack has root radius of 0.5 mm in both images.

The UMAT H-diff was then used to determine the hydrogen concentration at the crack tip as a function of the internal hydrogen pressure, 3.5 MPa (500 psi) and 43.8 MPa (6350 psi), and the elastic-plastic deformation response resulting from each loading condition. Model predictions for the hydrogen coverage are provided in Fig. 2b. Coupling the hydrogen-concentration prediction from ABAQUS and the phenomenological HA-FCG model described above, predictions of cycles to failure have been generated, based the size of the initial thumbnail-shaped crack. The model predictions, shown as a blue line, are compared to the experimental results of [26], in Fig. 3. The model accurately predicts the cycles to failure of the 4130 pressure vessels tested in [25] within a factor of 2 and is currently being updated for use with other pipeline and pressure vessel steels of interest.
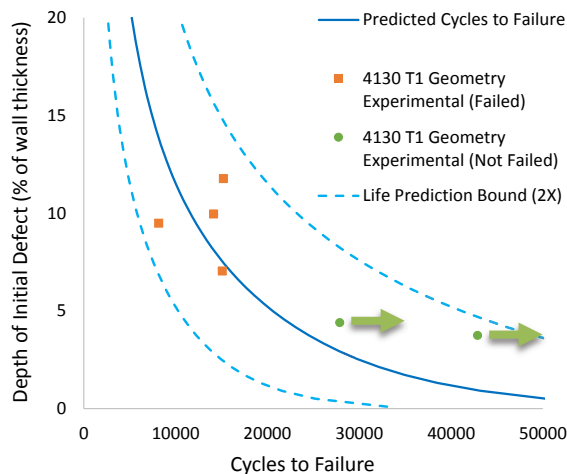
Figure 3: Cycles to failure for internal, thumbnail-shaped cracks in pressure vessels. HA-FCG predictions and experimental results as a function of initial crack size.

610

CONCLUSIONS

A coupled HA-FCG model framework has been implemented that accurately predicts the cycles to failure of laboratory specimens and realistic pipe and pressure vessel geometries. The current model implementation requires minimal calibration to steels of interest (Tables 1 and 2). The strength of this current model implementation is in its ability to predict HA-FCG for many grades of steel and geometries of interest.

REFERENCES

1. Park, G.T., Koh, S. U., Jung, H. G., Kim, K. Y., *Effect of microstructure on the hydrogen trapping efficiency and hydrogen induced cracking of linepipe steel.* Corrosion Science, 2008. **50**(7): p. 1865-1871.
2. Luppo, M.I., Ovejero-Garcia, J., *The influence of microstructure on the trapping and diffusion of hydrogen in a low carbon steel.* Corrosion Science, 1991. **32**(10): p. 1125-1136.
3. Chan, S.L.I., *Hydrogen Trapping Ability of Steels with Different Microstructures.* Journal of the Chinese Institute of Engineers, 1999. **22**(1): p. 43-53.
4. Dong, C.F., Liu, Z. Y., Li, X. G., Cheng, Y. F., *Effects of hydrogen-charging on the susceptibility of X100 pipeline steel to hydrogen-induced cracking.* International Journal of Hydrogen Energy, 2009. **34**(24): p. 9879-9884.
5. *United States Energy Information Administration, About U.S. Natural Gas Pipelines.* 2016 7/24/2016]; Available from: www.eia.gov/pub/oil_gas/natural_gas/analysis_publications/ngpipeline/index.html.
6. *U.S. Department of Energy, Energy Eficiency & Renewable Energy, Alternative Fuels Data Center, Hydrogen Production and Distribution*. 2016 7/24/2016]; Available from: www.afdc.energy.gov/fuels/hydrogen_production.html#distribution.
7. *U.S. Office of Energy Efficiency & Renewable Energy, ENERGY.gov, Hydrogen Pipelines*. 2016; Available from: http://energy.gov/eere/fuelcells/hydrogen-pipelines.
8. Somerday, B., P., *Technical Reference on Hydrogen Compatibility of Materials- Plain Carbon Ferritic Steels: C-Mn Alloys (Code 1100).* 2008, Sandia National Laboratories, Livermore, CA. p. 32.
9. Nanninga, N.E., Levy, Y. S., Drexler, E. S., Condon, R. T., Stevenson, A. E., Slifka, A. J., *Comparison of hydrogen embrittlement in three pipeline steels in high pressure gaseous hydrogen environments.* Corrosion Science, 2012. **59**(0): p. 1-9.
10. *B31.12 Hydrogen Piping and Pipelines*. 2014, American Society of Mechanical Engineers.
11. *ANSI/CSA CHMC 1-2014 Test Methods for Evaluating Material Compatibility in Compressed hydrogen Applications- Metals*. 2014, CSA Group: Ontario, Canada.
12. *ISO 11114-4:2005 Transportable Gas Cylinders- Compatibility of Cylinder and Valve Materials and Gas Contents*. 2005, ISO: Switzerland.
13. Slifka, A.J., Drexler, E. S., Nanninga, N. E., Levy, Y. S., McColskey, J. D., Amaro, R. L., Stevenson, A. E., *Fatigue crack growth of two pipeline steels in a pressurized hydrogen environment.* Corrosion Science, 2014. **78**(0): p. 313-321.
14. Drexler, E.S., Slifka, A. J., Amaro, R. L., Barbosa, N., Lauria, D. S., Hayden, L. E., Stalheim, D. G., *Fatigue crack growth rates of API X70 pipeline steel in a pressurized hydrogen gas environment.* Fatigue & Fracture of Engineering Materials & Structures, 2014. **37**(5): p. 517-525.
15. San Marchi, C., and Somerday, B.P. *Technical reference on hydrogen compatibility of materials: Plain carbon ferritic steels: C-Mn alloys (code 1100).* 2010 October 2010 [cited 2012 January 3, 2012]; Available from: http://www.sandia.gov/matlsTechRef/.
16. Amaro, R.L., Rustagi, N., Findley, K. O., Drexler, E. S., Slifka, A. J., *Modeling the fatigue crack growth of X100 pipeline steel in gaseous hydrogen.* International Journal of Fatigue, 2014. **59**(0): p. 262-271.

17.   Amaro, R.L., Drexler, E. S., Slifka, A.J., *Fatigue crack growth modeling of pipeline steels in high pressure gaseous hydrogen.* International Journal of Fatigue, 2014. **62**: p. 249-257.

18.   Amaro, R.L., Drexler, E. S., Slifka, A. J. *Development of an Engineering-Based Hydrogen-Assisted Fatigue Crack Growth Design Methodology for Code Implementation*. in *ASME 2014 Pressure Vessel and Piping Conference*. 2015. Anaheim, CA.

19.   Moriconi, C., G. Henaff, and D. Halm, *Influence of hydrogen coverage on the parameters of a cohesive zone model dedicated to fatigue crack propagation.* Procedia Engineering, 2011. **10**(0): p. 2657-2662.

20.   Novak, P., Yuan, R., Somerday, B. P., Sofronis, P., Ritchie, R. O., *A statistical, physical-based, micro-mechanical model of hydrogen-induced intergranular fracture in steel.* Journal of the Mechanics and Physics of Solids, 2010. **58**(2): p. 206-226.

21.   Sofronis, P., McMeeking, R. M., *Numerical analysis of hydrogen transport near a blunting crack tip.* Journal of the Mechanics and Physics of Solids, 1989. **37**(3): p. 317-350.

22.   Oriani, R.A., *The diffusion and trapping of hydrogen in steel.* Acta Metallurgica, 1970. **18**(1): p. 147-157.

23.   Kumnick, A.J., Johnson, H. H., *Deep trapping states for hydrogen in deformed iron.* Acta Metallurgica, 1980. **28**(1): p. 33-39.

24.   Boller, C., Seeger, T., *Materials Data for Cyclic Loading. Part B: Low-Alloy Steels*. Materials Science Monographs, 42B. 1987, Amsterdam, The Netherlands: Elsevier Science Publishers.

25.   San Marchi, C., Dedrick, D. E., Van Blarigan, P., Somerday, B. P., Nibur, K. A., *Pressure Cycling of Type 1 Pressure Vessels with gaseous Hydrogen*, in *Fourth International Conference on Hydrogen Safety*. 2011: San Francisco, CA.

26.   San Marchi, C., Harris, A., Yip, M., Somerday, B. P., Nibur, K. A. *Pressure Cycling of Steel Pressure Vessels with Gaseous Hydrogen*. in *ASME 2012 Pressure Vessels & Piping Conference, PVP2012-78709*. 2012. Toronto, Ontario, Canada: American Society of Mechanical Engineers.

Materials Performance in Hydrogen Environments

Proceedings of the 2016

International Hydrogen Conference

September 11-14, 2016

Jackson Lake Lodge, Wyoming, USA

Edited by

B.P. Somerday

P. Sofronis